Association genetics and genomic prediction for resistance to root rot in a diverse collection of Pisum sativum L.

Daniel Ariza-Suarez[1], Lukas Wille[1], Pierre Hohmann[2], Valentin Gfeller[2], Michael Schneider[2], Matthew Horton[2], Monika Messmer[2], and Bruno Studer[1]

[1]Eidgenossische Technische Hochschule Zurich Institut fur Agrarwissenschaften
[2]Forschungsinstitut fur Biologischen Landbau

September 02, 2024

Abstract

Root rot is one of the most threatening diseases to pea production. Root rot is caused by several interacting soil-borne pathogens, which makes it challenging to manage. Breeding for resistance is a promising approach for sustainable pea production. While quantitative trait loci (QTL) for resistance against individual pathogens have been identified, the genetic basis underlying resistance against the pathogen complex is poorly understood. Using a previously described diverse panel of 254 pea genotypes and 18k single nucleotide polymorphism (SNP) markers, we identified a novel QTL for resistance to root rot on chromosome chr6LG2. This QTL co-locates with a *mitochondrial Rho GTPase* and an *F-box* gene model, which are promising candidates for disease control. A whole-genome prediction model explained up to 53% of the phenotypic variation and reached predictive abilities of up to 0.51 for root rot-related traits. We found that plant height and shoot biomass were unreliable plant health indicators. Instead, these traits were related to the Mendelian *Le* locus, which controls stem length. Our results provide new insights into the genetic basis of quantitative root rot resistance in pea and provide novel tools that could accelerate the development of resistant pea lines through marker-assisted and genomic selection.

Daniel Ariza-Suarez[1], Lukas Wille[1,2], Pierre Hohmann[2,3], Valentin Gfeller[2], Michael Schneider[2], Matthew W. Horton[2], Monika M. Messmer[2*], Bruno Studer[1*]

[1]Molecular Plant Breeding, Institute of Agricultural Sciences, ETH Zurich, Zurich, Switzerland.

[2]Department of Crop Sciences, Research Institute of Organic Agriculture (FiBL), Frick, Switzerland.

[3]Department of Biology, Healthcare and the Environment, Faculty of Pharmacy and Food Sciences, Universitat de Barcelona, 08028 Barcelona, Spain.

[*]**Correspondence:** bruno.studer@usys.ethz.ch - monika.messmer@fibl.org

Author ORCIDs:

Daniel Ariza-Suarez: 0000-0002-1871-3514

Lukas Wille: 0009-0004-4090-3826

Pierre Hohmann: 0000-0001-7029-0566

Valentin Gfeller: 0000-0001-8896-7280

Michael Schneider: 0000-0002-6491-8852

Matthew W. Horton: 0000-0002-7537-0730

Monika M. Messmer: 0000-0002-6120-0079

Bruno Studer: 0000-0001-8795-0719

Keywords: Genome-wide association studies, genomic prediction, candidate resistance genes, pea (*Pisum sativum* L.), root rot.

Summary statement

Using association genetics in a diverse collection of pea genotypes, novel QTL, candidate genes and good genomic prediction abilities for resistance to root rot were identified, enabling genomics-assisted resistance breeding.

Introduction

Pea (*Pisum sativum* L.) is an important pulse crop for human consumption. Globally, around 14,166 Mt of dry peas were produced in 2022, ranking third after common bean and chickpea production (FAO, 2024). Pea production has also played a long-standing role in the European food system, but has declined since 1990 (FAO, 2024; Zander et al., 2016). Given its desirable nutritional quality and ability to fix nitrogen, pea has the potential to play a central role in healthy and sustainable human diets, as well as reducing greenhouse gas emissions associated with mineral fertilizer use (Cusworth et al., 2021). However, one of the most threatening factors for pea production are soil-borne diseases. (Jha et al., 2021). These include root rot caused by a complex of fungal and oomycete species such as *Aphanomyces euteiches* ,*Fusarium solani* , *Fusarium avenaceum* , *Fusarium graminearum* , *Thielaviopsis* spp., *Rhizoctonia* spp., and*Pythium* spp. (Rubiales et al., 2023; Wohor et al., 2022), also referred to as the pea root rot complex. These pathogens are responsible for severe seed and root rot, damping-off and seedling blight, leading to strong yield reductions (Rubiales et al., 2019). Management of root rot generally uses a combination of crop rotation and planting of certified and fungicide-treated seeds (Gossen et al., 2016). However, the disease remains a threat to pea production. In this sense, breeding for resistant genotypes is seen as a sustainable approach for controlling root rot in pea (Lamichhane et al., 2017; Pandey et al., 2021).

Breeding for resistance to root rot is a complex task. The phenotypic expression of the disease and the inheritance of resistance exhibit a quantitative behavior (Shehata et al., 1983; Wille et al., 2020). In addition, the root microbiome plays an important role in plant health by developing pathogenic, mutualistic or commensal interactions with the plant host (Bai et al., 2022). However, partial resistance has been reported in some pea genotypes (Jha et al., 2021), and molecular tools have been useful in exploiting resistance QTL for plant breeding. For example, marker-assisted backcrossing resulted in near-isogenic lines carrying single or combined alleles from different resistance QTL to*A. euteiches* (Lavaud et al., 2015). This is a significant advancement, as selecting for quantitative disease resistance is often related to durability but is difficult to achieve (Cowger & Brown, 2019; Nelson et al., 2018; Pilet-Nayel et al., 2017). Moreover, the recent availability of high-quality reference genomes is facilitating the identification of favorable alleles underlying phenotypic variation and accelerating breeding against root rot through genomics-assisted selection (Kreplak et al., 2019; Yang et al., 2022).

Several studies have reported the identification of multiple QTL for individual resistance to either *A. euteiches, F. solani* ,*F. avenaceum* or *F. graminearum* (Jha et al., 2021; Leprévost et al., 2023; Williamson-Benavides et al., 2021; Wu et al., 2021, 2022). While these studies have been an important step towards implementing more efficient resistance breeding strategies, they have some limitations. First, these studies relied on screening assays in which a single or a few isolates of individual pathogens were inoculated onto sterile substrates. While those protocols favor the reproducibility of results, they often fail to reflect real on-farm conditions where complex interactions between the plant and the microbiome contribute to plant

resistance (Wille et al. 2019). Second, most of these QTL were identified in biparental mapping populations, where the allelic diversity in such diploid, autogamous species is limited. Further, biparental QTL studies often have a limited mapping resolution and require the introgression of the beneficial resistance allele into breeding-relevant germplasm. Finally, most of these studies were carried out in the absence of a high-quality reference genome. Therefore, efficient exploitation of these QTL to accelerate disease resistance breeding has been limited. In fact, the genes involved in resistance to root rot are largely unknown, and only recent studies have highlighted the identification of candidate genes (Kälin et al., 2024). The use of a globally diverse panel of genotypes in an experimental setup with naturally infested soils could provide new insights into the resistance mechanisms of root rot and present new robust candidate loci for use in marker-assisted and genomic selection.

The main goal of this study was to characterize the genetic basis of root rot resistance in pea in a diverse collection previously described for quantitative resistance. To this end, we aimed to *i*) identify QTL and their underlying candidate genes associated with disease resistance using the recently available genomic resources; *ii*) compare different surrogate measures of plant health for association mapping and *iii*) explore the use of a whole-genome regression model to complement the association mapping approach and validate its use for genomic prediction purposes.

Materials and Methods

Plant material and phenotypic data

This study used the plant material and phenotypic results reported by Wille et al. (2020). Briefly, a panel of 261 pea genotypes was assembled and tested for resistance to root rot. The panel contained full-leaf and semi-leafless genotypes comprising 177 genebank accessions from the USDA-ARS GRIN Pea Core Collection, 47 advanced breeding lines from a private organic breeding organization (Getreidezüchtung Peter Kunz, Switzerland) and 34 registered cultivars (cv.) from Europe (Supplementary Table 1). In addition, the cv. 'EFB.33' and 'Respect' were used as the resistant and susceptible control checks to root rot, respectively. The panel was grown in pots with naturally infested soil (NS) and sterilized soil (S) under controlled conditions in a growth chamber with four replicates. Plant height and shoot dry weight (SDW) were measured to assess the overall performance of the plants in the trial. The traits plant emergence and root-rot index (RRI: 1 = no symptoms; 6 = complete disintegration of the root system) under NS conditions, as well as the shoot dry-weight ratio between NS and S conditions ($SDW_{NS/S}$) were proposed to be used as surrogate measures to identify resistant genotypes. Plant emergence indicates resistance against damping-off, while RRI shows resistance of plants that managed to emerge, and $SDW_{NS/S}$ indicates tolerance to disease damage. In this study, we also included the ratio between root and shoot dry weight of the plants under NS conditions (RDW/SDW_{NS}), which has been a useful indicator of root rot susceptibility in pea (Conner et al., 2013). This trait is used in genetic and physiological studies as a measure of the partitioning of resources between roots for nutrient and water absorption, and shoots for light interception and photosynthesis. Broad sense heritabilities for each trait were calculated according to Wille et al. (2020).

Genotyping

The population was genotyped-by-sequencing (GBS) following the protocol proposed by Poland et al. (2012), using a combination of *Pst* I and*Msp* I as restriction enzymes. GBS libraries were prepared at the plateforme d'analyses génomiques of the Institut de Biologie Intégrative et des Systèmes (IBIS, Université Laval, Québec, Canada) with the following modifications: a BluePippin (Sage Scientific, Beverly, MA) was used to size the libraries before PCR amplification (elution set between 50 and 65 min, on a 2% gel). Libraries were normalized, pooled, and then denatured in 0.02N NaOH and neutralized using HT1 buffer. Plate barcoding was used to enable sequencing on a shared Illumina NovaSeq S4 lane as described in Colston-Nepali et al. (2019). Sequencing was performed at the Centre d'expertise et de services Genome Québec in Canada. The

pool was loaded at 225pM on an Illumina NovaSeq S4 lane using the Xp protocol according to the manufacturer's recommendations. The run was performed for 2x150 cycles (paired-end mode). A phiX library was used as a control and mixed with libraries at 1% level. Base calling was performed using RTA (RRID:SCR_014332; v3). The bcl2fastq2 software (RRID:SCR_015058; v2.20) was then used to demultiplex samples and generate FASTQ reads.

Sequence demultiplexing was performed with Stacks (RRID:SCR_003184; v2.60) (Catchen et al., 2013), allowing up to one mismatch in the adapter sequence. Adapter tails were clipped with HTStream (RRID:SCR_018354; v1.3.3) (https://github.com/s4hts/HTStream). Using Bowtie (RRID:SCR_016368; v2.4.4) (Langmead & Salzberg, 2012), the processed reads were mapped to the reference genomes of *P. sativum* cv. 'Caméor' (Kreplak et al., 2019) and 'Zhongwan 6' (Yang et al., 2022), hereafter referred to as Cam. and ZW6, respectively. The mapped reads were used for single nucleotide polymorphism (SNP) calling using NGSEP (RRID:SCR_012827; v4.1.0) (Tello et al., 2023). The genotypic matrix was filtered for genotype calls with a quality score above 30, minor allele frequency above 0.02, and a maximum observed heterozygosity rate of 0.05 per SNP marker. Finally, SNPs with less than 22% genotyped samples were removed to reduce the proportion of missing data in the genotypic matrix to approximately 30%. The predicted effect of these sequence variants on the gene models of the reference genomes was annotated with snpEff (RRID:SCR_005191; v5.0e) (Cingolani et al., 2012).

Population structure and linkage disequilibrium

Population structure and linkage disequilibrium (LD) analyses were performed using the reference genome Cam. Pairwise measures of LD were calculated for each chromosome in sliding windows of 100 markers using the final genotypic matrix. The LD measures were corrected for kinship relationships in the population (r_V^2) as implemented in the R package LDcorSV (v1.3.2) (Mangin et al., 2012). The LD decay was estimated regressing the pairwise r_V^2 values on the physical distance of their markers using the locally estimated scatterplot smoothing implemented in the R function 'loess' (v4.1.2), with a span value of 0.5. The population structure was assessed with a principal component analysis (PCA) using the genotypic matrix described above. Missing data in the matrix used for PCA was imputed using Beagle (RRID:SCR_001789; v5.2) (Browning et al., 2018), setting the effective population size to 1,000 and default parameters.

Genome-wide association studies and genomic prediction

Association mapping was performed for each quantitative trait using the linear mixed model approach implemented in the R package GENESIS (v2.24.0) (Gogarten et al., 2019). This model included three principal components and a kinship matrix to correct for population structure and relatedness. The association mapping on the binary trait leaf type was conducted using a generalized linear mixed model via the penalized quasi-likelihood approximation proposed by Chen et al. (2016) and implemented in the same R package GENESIS. Significant associations were defined when the p value for each SNP marker was smaller than the Bonferroni-corrected threshold, which was calculated with a genome-wide type I error rate of 0.05.

A Bayesian Ridge regression (BRR) model was fitted using the R package BGLR (v1.0.9) (Pérez & De Los Campos, 2014) with 10,000 iterations, using 1,000 as burn-in. In this model, all imputed SNP markers were included as predictors of the phenotypic data, with a Gaussian prior assigned to marker effects. The genomic heritability was calculated using the remaining iterations thinned by a factor of 5. It used the sample variance of genomic values at each iteration of the sampler, as described by de los Campos et al. (2015). The estimates of marker effects were extracted from the fitted model. The prediction ability of the model was assessed by 50 times cross validation, randomly splitting the dataset into training (70%) and validation (30%) subsets. Pearson's correlation coefficients between observed and predicted values of the validation subset were calculated to quantify the prediction ability for each trait.

Results

Genotyping, linkage disequilibrium and population structure analysis

Genotyping-by-sequencing yielded a SNP matrix with 17,266 and 18,489 sequence variants using Cam. and ZW6 as reference genomes, respectively, for 254 out of 261 individuals. These variants were evenly distributed along the seven chromosomes of the two reference genomes (Supplementary Figure 1). The population structure analysis of the SNP matrix revealed that the first and the second principal component accounted for 8.0% and 4.4% of the observed variance, respectively (Figure 1A). The projection of genotypes in the bidimensional space defined by these principal components revealed two major groups that can mainly be distinguished by origin of the seed: the accessions sourced from the USDA-ARS gene bank and the European breeding material. These two groups were close to each other and contained a few accessions overlapping with the other group. Using pairwise measures of LD between the SNP markers, the genome-wide LD decay was 1.5 Mbp at 0.077 r^2_V, half of its maximum value (Figure 1B). The LD decay rate was very similar among chromosomes, ranging between 1.2 Mbp at 0.091 r^2_V (chr1LG6) to 1.53 Mbp at 0.067 r^2_V (chr2LG1).

Phenotypic correlations

High phenotypic correlations ranging between 0.64 and 0.92 were observed for the early vigor-related traits plant height and SDW, as published by Wille et al. (2020) (Supplementary Figure 2). These high correlations were consistent for trials managed under NS and S conditions. High heritabilities were observed for the early vigor-related traits, ranging between 0.92 to 0.98. On the other hand, the phenotypic correlations among root rot-related traits were inconsistent, ranging from $SDW_{NS/S}$) to |-0.60| (RRI_{NS} vs. $SDW_{NS/S}$). The heritability for these traits was high only for plant emergence $_{NS}$(0.89), while the others showed lower values of 0.43 (RRI_{NS}) and 0.51 ($SDW_{NS/S}$). The correlations between early vigor and root rot-related traits did not show any clear pattern. They ranged between |0.46| (SDW_{NS} vs $SDW_{NS/S}$) and |-0.54| (RRI_{NS} vs. SDW_{NS}). The newly introduced variable RDW/SDW_{NS} did not show high correlations with any of the previously reported traits and had a heritability of 0.48.

Association mapping

The binary trait leaf type was associated with a single genomic region on chromosome chr2LG1, where the most significantly associated marker was located at 409,403,647 and 469,582,243 bp in the Cam. and ZW6 reference genomes, respectively (Figure 2, Table 1, Supplementary Figure 3 and Supplementary Table 2). The p value of this marker came close but did not reach the Bonferroni-corrected threshold of significance. A close examination of the distribution of this trait in the population revealed that the semi-leaf-less genotypes were almost exclusively present in the European breeding material (Figure 1). This likely reduced the power to identify significant associations due to population structure correction.

The early vigor traits plant height and SDW under NS and S conditions were associated with a single region in the distant arm of chromosome chr5LG3 between 565-580 Mbp and 637-660 Mbp in the Cam. and ZW6 reference genomes, respectively (Figure 2, Table 1 and Supplementary Figure 3). Closer examination of this region revealed at least three peaks in the associated genome region (Figure 3). The most significantly associated markers for plant height defined the first two subregions of association at 569,788,697 bp and 573,695,584 bp in the Cam., and 642,030,534 bp and 646,378,981 bp in the ZW6 reference genome. The estimated marker effects ranged from 4.64 to 6.87, and the proportion of variance explained (PVE) from 0.150 to 0.214 (Figure 3, Table 1, Supplementary Figure 4 and Supplementary Table 2). The SNPs PsCam_chr5LG3_569788697_G/T and PsZW6_chr5_642030534_C/A were located at the intron region of the gene models $Psat5g301400_{Cam.}$ | $Psat05G0828800_{ZW6}$, which encode a member of the Nucleoporin interacting component (Nup93/Nic96-like) family (74% sequence identity to AT2G41620.1 in *Arabidopsis thaliana*). The SNPs PsCam_chr5LG3_573695584_C/A and PsZW6_chr5_646378981_T/C were located at the intron region of the gene models $Psat5g304720_{Cam.}$ | $Psat05G0837000_{ZW6}$, which encode a homologue of the

Golgi SNARE 11 protein (GOS11; 80% sequence identity to AT1G15880.1 in *A. thaliana* , Supplementary Table 2). The most significantly associated markers for SDW_S and SDW_{NS}PsCam_chr5LG3_573520009_A/C and PsZW6_chr5_646205699_A/C were located within the second subregion of association, with an estimated effect between 0.02 - 0.03 g and PVE between 0.095 - 0.148 (Figure 3, Table 1, Supplementary Figure 4 and Supplementary Table 2). The third subregion was shared by all four traits and included the significantly associated markers PsCam_chr5LG3_577882635_T/C | PsZW6_chr5_652345014_T/C and PsCam_chr5LG3_577882853_A/G | PsZW6_chr5_652345232_A/G, with estimated effects between 3.14 - 4.44 cm and 0.012 - 0.022 g, and a PVE between 0.068 - 0.111 and 0.034 - 0.117, respectively (Supplementary Table 2).

The root rot-related traits plant emergence $_{NS}$, RRI_{NS} and $SDW_{NS/S}$ were concordantly associated with a single region in the proximal arm of chromosome chr6LG2. However, the newly introduced trait $RDW/SDW_{NS}$was not associated with any region of the genome (Figure 4, Table 1 and Supplementary Figure 5). All significantly associated markers for these traits were in strong LD within a region spanning approximately 10 kbp around 68.265 Mbp and 85.085 Mbp in the Cam. and ZW6 reference genomes, respectively (Figure 5). The estimated effects for the most significantly associated markers for $SDW_{NS/S}$, RRI_{NS} and emergence $_{NS}$ were 0.1, -0.21 and 0.135 and their PVE was 0.10, 0.08 and 0.15, respectively (Figure 5, Table 1, Supplementary Figure 6 and Supplementary Table 2). This region co-locates with the gene models $Psat6g060320_{Cam.}$| $Psat06G0169300_{ZW6}$, which encode a*mitochondrial Rho* (*MIRO*)-related GTPase. The markers PsCam_chr6LG2_68264764_T/C | PsZW6_chr6_85080362_G/T and PsCam_chr6LG2_68264779_G/T | PsZW6_chr6_85080347_T/C fall within the intron region of $Psat6g060320_{Cam.}$ | $Psat06G0169300_{ZW6}$, whereas the annotation of PsCam_chr6LG2_68269898_A/T | PsZW6_chr6_85085481_A/T predicts a synonymous mutation in the exon region of the same gene models (Supplementary Table 2).

Genomic prediction

The whole-genome regression model yielded variable results consistent with the broad sense heritability of each trait, but unaffected by the reference genome used (Table 2). The genomic heritabilities ranged between 0.25 (RRI_{NS}) and 0.84 (plant $height_S$). Similarly, the mean prediction ability of the BRR model ranged between 0.13 (RRI_{NS}) and 0.81 (plant $height_S$). The missing heritability, defined as the difference between broad sense and genomic heritability, showed less variation with values ranging between 0.14 (plant height $_S$) and 0.36 (emergence $_{NS}$). The estimated marker effects for root rot-related traits were larger for emergence $_{NS}$ (Figure 6 and Supplementary Figure 7). In line with the results of the genome-wide association studies (GWAS), the BRR model showed a SNP marker with large effects on chr6LG2 at 68.265 Mbp and 85.085 Mbp in the Cam. and ZW6 reference genomes, respectively. However, it also showed a SNP on chr4LG4 with comparable marker effects at 180.86 Mbp and 216.78 Mbp in the Cam. and ZW6 reference genomes, respectively. This region coincides with a non-significant peak in chr4LG4 observed for $emergence_{NS}$ (Figure 4 and Supplementary Figure 5). Other markers on chr3LG5, chr6LG2 and chr7LG7 showed minor effects for $emergence_{NS}$ (Figure 6 and Supplementary Figure 7). Taken together, all 17,266 and 18,489 SNP markers explained up to 51% and 53% of the observed phenotypic variance for $emergence_{NS}$ in the Cam. and ZW6 reference genomes, respectively (Table 2).

Discussion

A novel QTL and candidate genes for resistance to root rot in pea

Resistance to root rot in pea is of quantitative nature and has been studied for decades, resulting in the identification of multiple QTL across the genome (Jha et al., 2021). In this study, a single genomic region was consistently associated with the root rot-related traits on chromosome chr6LG2 at 68.265 Mbp and 85.085 Mbp in the Cam. and ZW6 reference genomes, respectively. Other QTL for root rot resistance in pea have

been reported on this chromosome: First, the moderate effect QTL AeMRCD1Ps-2.1 and AeMRCD1Ps-2.2 against A. euteiches were identified by Wu et al. (2021) between 404.587 and 465.936 Mbp (Cam.), with R^2 values of 14.3% and 13.8%, respectively. Second, the minor and major QTL Ae-Ps2.1 and Ae-Ps2.2 on chr6LG2 showed R^2 values of 15.4% and 26.9%, respectively (Hamon et al., 2011, 2013). However, the exact physical location of these QTL was not available (Pulse Crop Database - www.pulsedb.org; as of July 2024). Finally, the resistance QTL Fsp-Ps2.1 against F. solani was consistently identified by Coyne et al. (2015, 2019) with R^2 values between 57.1% and 72.2%.The neighboring markers of this QTL are located at 10.635 and 235,738 Mbp (Cam.; Pulse Crop Database - www.pulsedb.org; as of July 2024). The different physical locations of these markers suggest that these QTL are independent of each other. Taken together, our results indicate a narrow region on chr6LG2 that is not linked to any of these previously reported QTL. This novel QTL is consistent with the quantitative nature of resistance.

A few candidate genes have been proposed from the identification of multiple QTL for root rot resistance in legumes: For instance, three defensin genes were mapped together near the QTL Fsp-Ps3.1 identified on chr5LG3 (Coyne et al., 2015). These genes were upregulated upon F. solani infection in pea (Chiang & Hadwiger, 1991). Similarly, an F-box encoding gene (Medtr3g011020) was identified in the resistance of Medicago truncatula to A. euteiches (Bonhomme et al., 2014). More recently, a list of 39 candidate genes from transcriptomic analysis for Aphanomyces resistance was reported. These genes are distributed over all chromosomes, but the most promising were located on chr7LG7 (Kälin et al., 2024). Despite these examples, the molecular mechanisms underlying resistance to root rot in legumes are poorly understood to date (Cowger & Brown, 2019; Pilet-Nayel et al., 2017). In this study, the region of association on chromosome chr6LG2 coincides with the gene models Psat6g060320Cam. | Psat06G0169300ZW6 that encode a MIRO -related GTPase. Its peptide sequence is homologous to the gene models Lcu.2RBY.1g063750.1 (Lens culinaris), Medtr1g072280.1 (M. truncatula), and MIRO1 (AT5G27540.1; Arabidopsis thaliana), with 95, 83 and 54% sequence identity, respectively (Lamesch et al., 2012; Ramsay et al., 2021; Tang et al., 2014).

Research on plant Rho GTPases is still in its infancy. Yet, increasing evidence indicates that they play a critical role in plant immunity (Engelhardt et al., 2020; Kawano et al., 2014; Rivero et al., 2019). For example, silencing of the M. truncatula Rho of plant 9 (MtROP9) gene favored early root colonization by mycorrhizal fungi and A. euteiches (Kiirika et al., 2012). Consistent with these findings, the MIRO- related GTPase Medtr1g072280 was proposed as a candidate tolerance gene against the root lesion nematode Pratylenchus neglectus in Medicago littoralis (Oldach et al., 2014). However, some studies have shown that the homologue genes MIRO1 (AT5G27540) and MIRO2 (AT3G63150) in Arabidopsis are involved in salt stress response, embryogenesis, pollen tube growth, and mitochondrial development (Jayasekaran et al., 2006; Wang et al., 2008; White et al., 2020; Yamaoka & Leaver, 2008). In this sense, the mechanism by which a mitochondrial GTPase might be involved in root rot resistance is undetermined. Although the MIRO-related GTPases Psat6g060320Cam. | Psat06G0169300ZW6 have been consistently identified for three root rot-related traits in this study, it is still possible that the causal gene(s) or mutation(s) lies in the surrounding region. Indeed, the gene models Psat6g063320Cam. | Psat06G0173100ZW6 are the pea homologues of the F-box gene (Medtr3g011020) identified in M. truncatula resistance to A. euteiches (Bonhomme et al., 2014). This gene is located 2.22 Mbp downstream of the association region on chr6LG2 and is also a plausible candidate. Similarly, the defense response candidate genes Psat6g042720Cam., Psat6g042840Cam. and Psat6g043800Cam. identified by Kälin et al. (2024) are located approximately 30 Mbp upstream of the association region containing the MIRO -related GTPases.

The quantitative nature of resistance to root rot is supported by multiple QTL

Whole-genome regression and GWAS models, despite their similarities, serve different purposes in breeding (Legarra et al., 2018; Zhang et al., 2021). Our GWAS results point to a single QTL in chr6LG2, which accounts for a moderate proportion of the phenotypic variability for root rot-related traits. Given the genotypic variation and inconsistent phenotypic correlations between these traits, suggesting different genetic control mechanisms for resistance (Wille et al., 2020), we used a whole-genome regression model to supplement

GWAS results. This model showed subtle marker effects in the region of association in chr6LG2 for RRINS and SDWNS/S, which limits conclusions about their genetic control. However, markers with the highest estimated effects for plant emergence NS, the trait with the highest disease resistance heritability, coincide with the region of association on chr6LG2. Markers on chr4LG4 at 180.86 Mpb (Cam.) and 216.78 Mbp (ZW6) have comparable effects, with other markers on chr6LG2, chr3LG5 and chr7LG7 having smaller effects. The variance explained by all 18k markers (0.51Cam. – 0.53ZW6) exceeds that of the most significantly associated markers identified by GWAS (0.16Cam. – 0.15ZW6). This underlines the importance of other QTL with moderate and small effects on root rot resistance in pea. In fact, the region on chr4LG4 is near the moderate-effect QTL Fg-Ps4.1 (202,652,401-234,329,355 bp in Cam.) and Fg-Ps4.2 (184,181,231-194,948,669 bp in Cam.) reported against F. graminearum (Wu et al., 2022). The major-effect QTL Ae-Ps4.5 was recently fine-mapped to a 3.06 Mbp interval in chr4LG4 (296,700,000 – 299,750,000 bp in Cam.) (Lavaud et al., 2024). Similarly, other minor resistance QTL have been reported on chr3LG5, chr4LG4, chr6LG2 and chr7LG7 (Coyne et al., 2019; Desgroux et al., 2018; Jha et al., 2021; Wu et al., 2021). In addition, the whole-genome regression model achieved a predictive ability of up to 0.51 for plant emergence NS. This could be useful for implementing genomic selection strategies to improve root rot resistance in a pea breeding program (Rubiales et al., 2023), as has been demonstrated for root rot diseases in common bean (Diaz et al., 2021).

Early vigor QTL were related to the Le locus, not root rot resistance

Plant height is a morphological trait for which high heritabilities and predictive abilities were reported in pea (Bari et al., 2021; Wille et al., 2020; Wu et al., 2021). We identified a genomic region between 565-580 Mbp and 637-660 Mbp on chr5LG3 in the Cam. and ZW6 reference genomes, respectively, associated with plant height and SDW under NS and S conditions. Several studies reported the identification of QTL associated with plant height on chr5LG3. These include the QTL HT-Ps3.1 , located at 493,071 Mbp in the Cam. reference genome (Hamon et al., 2013); the QTL WB.FspPs5.2 and WB.FspPs5.1 , located between 516-569 Mbp and 236-296 Mbp, respectively (Williamson-Benavides et al., 2021); and a QTL from a GWAS located between 566-573 Mbp in the same genome (Gali et al., 2019), which is consistent with the results presented in this study. In line with our results for SDW, Burstin et al. (2007) and Klein et al. (2014) reported QTL in LG3 that are associated both with reduced plant height and vegetative biomass, whereas Wu et al. (2021) found no association on chr5LG3 for dry foliage weight. Some of these studies link the identified QTL to the well-known Le locus that controls internode length in pea (Mendel, 1866). This locus encodes a gibberellin 3β-hydroxylase that controls the 3β-hydroxylation of gibberellin A20 to gibberellin A1 (Martin et al., 1997). A BLAST search on the peptide sequence of this protein reveals that it corresponds to the gene models Psat5g299720Cam. | Psat05G0825300ZW6. These models are located approx. 2.42 Mbp upstream of the most significantly associated markers for plant height PsCam_chr5LG3_569788697_G/T | PsZW6_chr5_642030534_C/A identified in this study.

Various surrogate traits have been used to evaluate root rot in pea plants under controlled conditions, such as disease severity-related indices, biomass of shoot and root sections of the plant, or plant height and vigor (Bodah et al., 2016; Conner et al., 2013; Desgroux et al., 2018). The results presented in this study show that early vigor and root rot-related traits have independent associations on chromosomes chr5LG3 and chr6LG2, respectively. These observations match previous findings, showing that plant height is a poor measure of root rot severity in pea (Wu et al., 2021, 2022), while they also challenge other reports where plant height was more closely related to disease severity (Bodah et al., 2016; Williamson-Benavides et al., 2021). In parallel, our results highlight the caution in using SDW (i.e. SDWNS or SDWS) as a root rot-related trait, as it showed stronger relationships with plant height and not disease resistance. Instead, RRINS, SDWNS/S and plant emergence NS provided a predictable measurement of the plant health (Wille et al., 2020), yielding consistent associations in the genome. Finally, the newly introduced root-shoot ratio trait RDW/SDWNS was reported to be a useful indicator of plant susceptibility to root rot (Conner et al., 2013). In this study, it presented moderate broad sense heritability and low phenotypic correlation with root rot-related traits. These characteristics made it a suitable prospect to further elucidate the genetic basis controlling the resistance against root rot. However, no significant association was observed for this trait

which undermined its potential as a surrogate of plant health.

The afila locus is not related to root rot resistance in pea

In pea, the semi-dwarf, semi-leafless type is characterized by superior standing ability, less favorable conditions for pests and foliar diseases and unaffected yield performance compared to full-leaf types (Mikić et al., 2011; Sinjushin et al., 2022). These features make it an important achievement of pea breeding (Tayeh et al., 2015). The semi-leafless type was obtained by the introduction of the afila (af) mutation with retained full-type stipules. af has been studied for several decades and is on LG1 of different genetic linkage maps reported for pea (Ellis et al., 1992). In this study, the presence-absence of semi-leafless types in the population was similarly associated to a region in the distant arm of chr2LG1, at 409 Mbp and 469 Mpb in the Cam. and ZW6 reference genomes, respectively. This region is 3 Mbp downstream of a region containing two PALMATE-LIKE PENTAFOLIATA 1s (PsPALM1a and PsPALM1b), whose deletion is reported to be associated to the af mutation (Tayeh et al., 2024; Yuan et al., 2024). Previous reports have shown that a DNA marker for af segregated with the resistance QTL Ae-Ps1.2 , where the resistance allele is in coupling phase with the full-leaf type allele (Hamon et al., 2011). In fact, this allele was later proposed as a pleiotropy marker affecting leaf morphology and Aphanomyces resistance (Hamon et al., 2013). However, we did not find any association on chr2LG1 for root rot-related traits. 1 Discussion

Concluding remarks

In this work, we identified a novel QTL for resistance to root rot caused by a pathogenic complex present in infested soil. We used data from a diverse collection of pea genotypes grown in naturally infested soil. This approach brings experimental and on-farm conditions closer together, facilitating their application in real breeding contexts. Our results provide a promising opportunity for implementing marker-assisted and genomic selection strategies to improve root rot resistance in pea breeding schemes. While this study considered the effect of the entire microbiome and pathobiome, the analyses to identify genomic regions associated with resistance to root rot focused only on plant traits. However, the microbiome composition may substantially contribute to the ability to predict resistance. Further research should address the effect of the rhizosphere microbial community on root rot. This could provide additional tools that can be incorporated into the selection process in a breeding program.

Acknowledgments

We thank the interns and technicians of FiBL and ETH Zurich for plant cultivation and DNA extraction, Klaus Oldach (KWS LOCHOW GMBH) and Steven Yates (ETH Zurich) for the valuable inputs and interesting discussions, which helped to improve the content of this work, and Jean-Claude Walser from the Genetic Diversity Centre (GDC) of ETH Zurich for downloading and storing the raw sequencing data produced in this study. The sequencing data was processed and analyzed on the Euler cluster of ETH Zurich.

Figures and tables

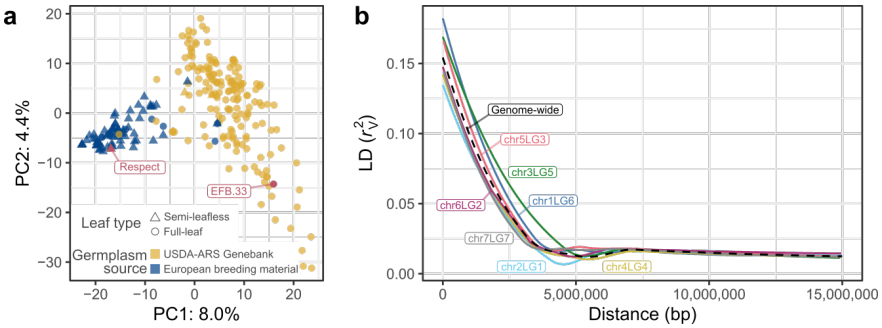

Figure 1 (a) Population structure assessment using principal component analysis of single nucleotide polymorphism (SNP) data. The location of each genotype is represented by a point in the two-dimensional space defined by the first and second principal component (PC). The color of the points represents the germplasm source, while the shape represents their leaf type. The red tagged points show the location of the cv. 'EFB.33' and 'Respect', the resistant and susceptible control checks used in the growth chamber trial, respectively. (b) Patterns of linkage disequilibrium (LD) decay calculated genome-wide (black-dashed line) and for each chromosome separately (colored lines) from SNP data. Each line corresponds to a locally estimated scatterplot smoothing (LOESS) regression on the LD measures.

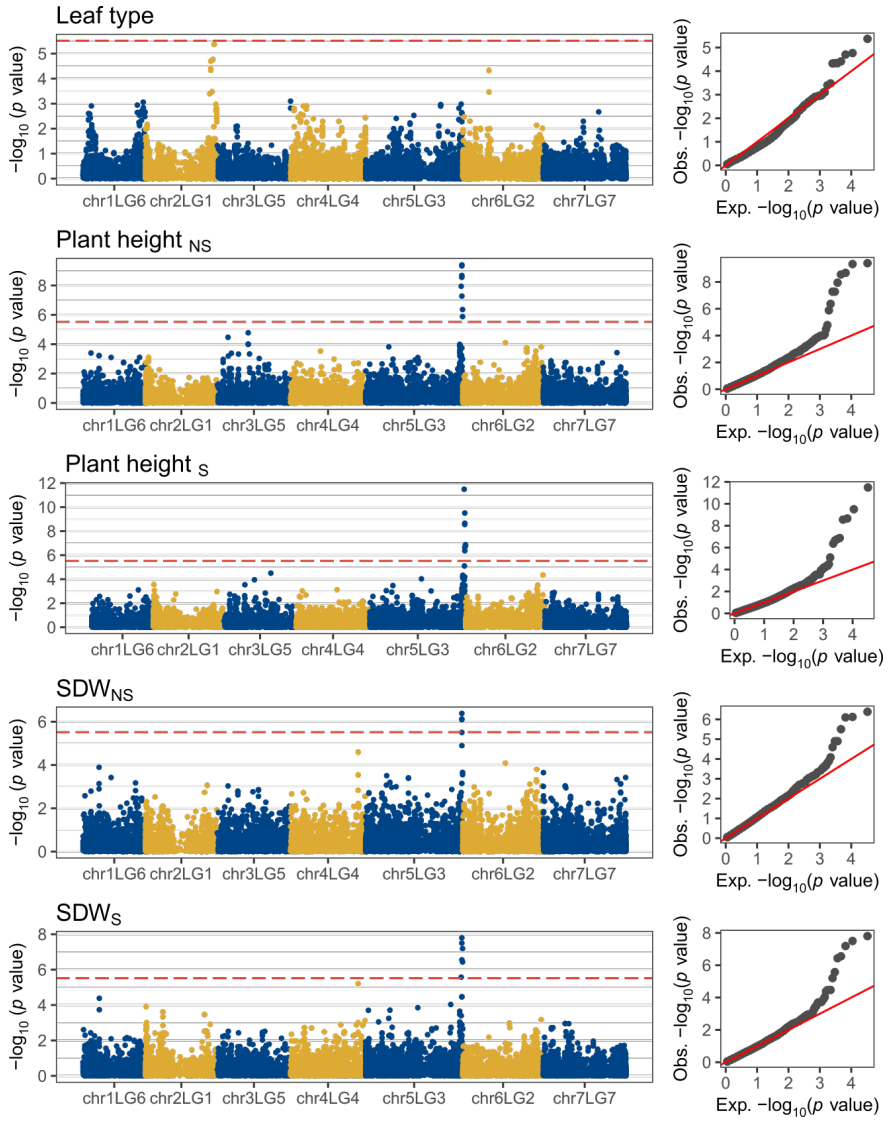

Figure 2 Results of the genome-wide association studies for the traits leaf type, plant height and shoot dry weight (SDW) under naturally infested (NS) or sterilized soil conditions (S). The horizontal, red-dashed line represents the Bonferroni-corrected threshold, which was calculated with a genome-wide type I error rate of $\alpha = 0.05$ ($p < 2.028 \times 10^{-6}$). The results are presented as individual Manhattan plots, showing the significance of the single nucleotide polymorphisms (SNP) and their physical location on each of the seven chromosomes of the reference genome of cv. 'Caméor'. The corresponding quantile-quantile-plots to the right compare the deviation between the observed and the expected significance of the SNP from a theoretical X^2 distribution.

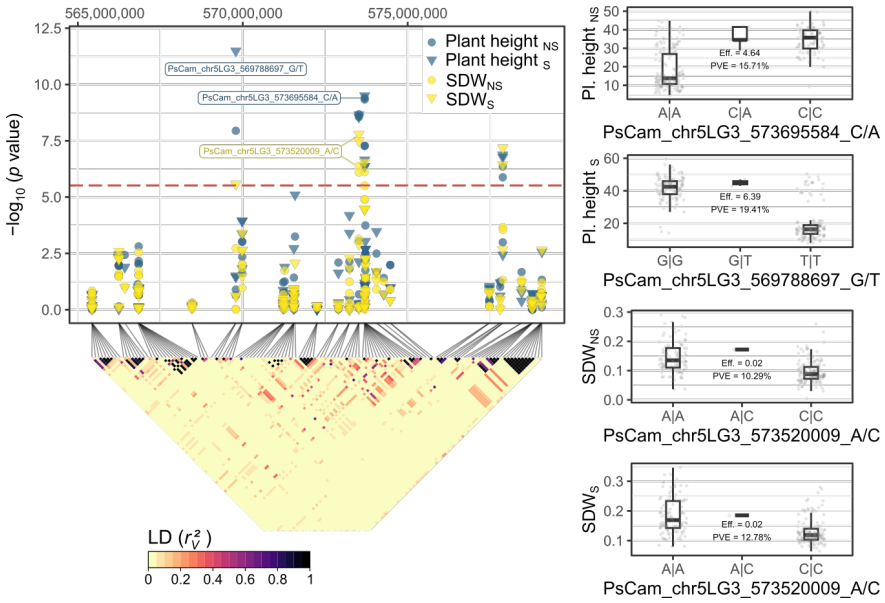

Figure 3 Genetic dissection of the region of association on chromosome chr5LG3 for the traits plant height and shoot dry weight (SDW) under naturally infested (NS) and sterilized (S) soil conditions. The scatterplot shows combined results of individual genome wide association studies (GWAS). Each point shows the significance of sequence variants (SNP) and their physical location on chr5LG3 of the genome of cv. 'Caméor'. The horizontal, red-dashed line represents the Bonferroni-corrected threshold, which was calculated with a genome-wide type I error rate $\alpha = 0.05$ ($p < 2.028 \times 10^{-6}$). The tagged points indicate the most significant SNPs for each trait. The colored square matrix below represents the pairwise linkage disequilibrium (LD) measurements ($\mathbf{r^2}$) between each pair of SNPs in the region of association. The boxplots show the distribution of phenotypic values between the genotypes of the most significant SNPs on chr5LG3. Each plot includes the marker effect (Eff.) and the proportion of variance (PVE) derived from the GWAS model.

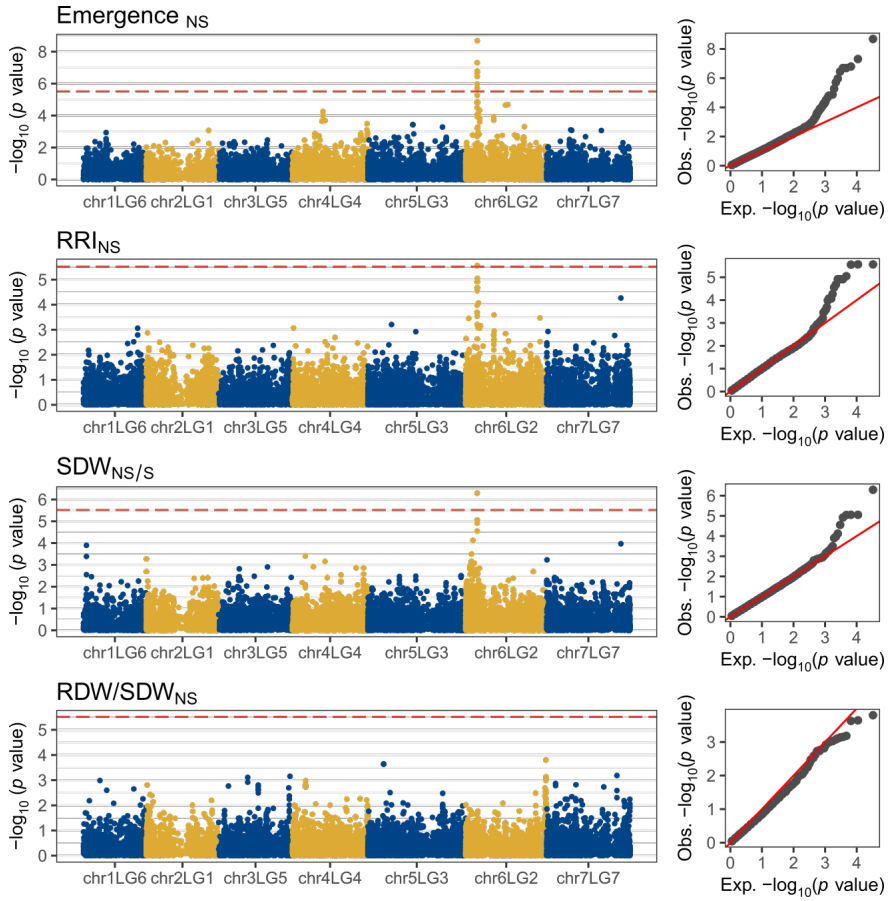

Figure 4 Results of the genome-wide association studies for the root rot-related traits plant emergence and root rot index (RRI) under naturally infested soil conditions (NS), shoot dry weight (SDW) ratio between naturally infested and sterilized soil conditions (NS/S), and the ratio between root and shoot dry weight (RDW/SDW) under NS conditions. The horizontal, red-dashed line represents the Bonferroni-corrected threshold, which was calculated with a genome-wide type I error rate $\alpha = 0.05$ ($p < 2.028 \times 10^{-6}$). The results are presented as individual Manhattan plots showing the significance of the sequence variants (SNP) and their physical location on each of the seven chromosomes of the reference genome of cv. 'Caméor'. The corresponding quantile-quantile-plots to the right compare the deviation between the observed and the expected significance of the SNP from a theoretical X^2 distribution.

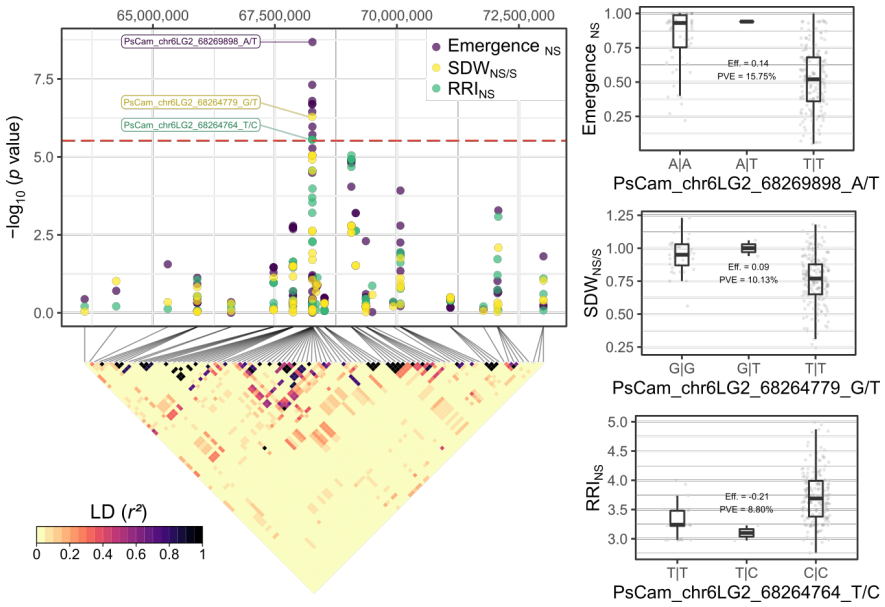

Figure 5 Genetic dissection of the region of association on chromosome chr6LG2 for the root rot-related traits plant emergence, root rot index (RRI) and shoot dry weight (SDW) under naturally infested (NS) and sterilized (S) soil conditions. The scatterplot shows combined results of individual genome wide association studies (GWAS). Each point shows the significance of sequence variants (SNP) and their physical location on chr6LG2 in the genome of cv. 'Caméor'. The horizontal, red-dashed line represents the Bonferroni-corrected threshold, which was calculated with a genome-wide type I error rate $\alpha = 0.05$ ($p < 2.028 \times 10^{-6}$). The tagged points indicate the most significant SNPs for each trait. The colored square matrix below represents the pairwise linkage disequilibrium (LD) measurements (r^2) between each pair of SNPs in the region of association. The boxplots show the distribution of phenotypic values between the genotypes of the most significant SNPs on chr5LG3. Each plot includes the marker effect (Eff.) and the proportion of variance (PVE) derived from the GWAS model.

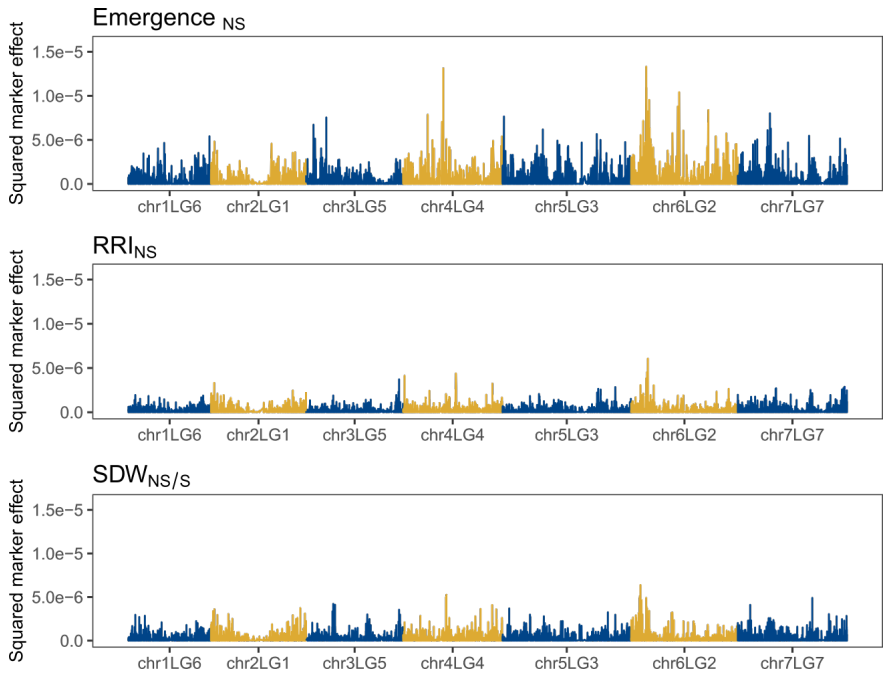

Figure 6 Sequence variant (SNP) effects derived from a Bayes ridge regression model that used all SNP markers as predictors of root rot-related traits plant emergence and root rot index (RRI) under naturally infested soil conditions (NS), shoot dry weight (SDW) ratio between naturally infested and sterilized soil conditions (NS/S). The squared marker effects are plotted along their physical position on each one of the seven chromosomes of the reference genome of cv. 'Caméor'.

Table 1 Genome-wide association results for the most significantly associated markers with leaf type, plant height, shoot and root dry weight (SDW and RDW, respectively), plant emergence and root rot index (RRI) evaluated under naturally infested or sterilized soil conditions (NS and S, respectively). The physical location of each marker is given by the chromosome (Chr.) and position (Pos.) in the reference genome of cv. 'Caméor' or 'Zhongwan 6'. The level of significance (p value), the proportion of variance explained (PVE) and the estimated effect (Est. effect) of each marker were obtained from the corresponding mixed model used for association.

Trait	**Ref. genome**	**SNP ID**	**Chr.**	**Pos. (bp)**	p **value**	**PVE**	**Es**
Leaf type	Caméor	PsCam_chr2LG1_409403647_G/A	chr2LG1	409,403,647	4.26E-06	0.287	2.1
	Zhongwan 6	PsZW6_chr2_469582243_G/A	chr2	469,582,243	1.40E-05	0.269	2.0
Plant height $_{NS}$	Caméor	PsCam_chr5LG3_573695584_C/A	chr5LG3	573,695,584	3.97E-10	0.157	4.6
	Zhongwan 6	PsZW6_chr5_646378981_T/C	chr5	646,378,981	9.39E-10	0.15	5.3
Plant height $_{S}$	Caméor	PsCam_chr5LG3_569788697_G/T	chr5LG3	569,788,697	3.25E-12	0.194	6.3
	Zhongwan 6	PsZW6_chr5_642030534_C/A	chr5	642,030,534	2.52E-13	0.214	6.8
SDW_{NS}	Caméor	PsCam_chr5LG3_573520009_A/C	chr5LG3	573,520,009	4.13E-07	0.103	0.0
	Zhongwan 6	PsZW6_chr5_646205699_A/C	chr5	646,205,699	1.10E-06	0.095	0.0
SDW_{S}	Caméor	PsCam_chr5LG3_573520009_A/C	chr5LG3	573,520,009	1.58E-08	0.128	0.0
	Zhongwan 6	PsZW6_chr5_646205699_A/C	chr5	646,205,699	1.19E-09	0.148	0.0
RRI_{NS}	Caméor	PsCam_chr6LG2_68264764_T/C	chr6LG2	68,264,764	2.73E-06	0.088	-0.2
	Zhongwan 6	PsZW6_chr6_85080347_T/C	chr6	85,080,347	4.32E-06	0.084	-0.2
$SDW_{NS/S}$	Caméor	PsCam_chr6LG2_68264779_G/T	chr6LG2	68,264,779	5.11E-07	0.101	0.0
	Zhongwan 6	PsZW6_chr6_85080362_G/T	chr6	85,080,362	1.07E-07	0.113	0.1

Trait	Ref. genome	SNP ID	Chr.	Pos. (bp)	p value	PVE	Es
Plant emergence $_{NS}$	Caméor	PsCam_chr6LG2_68269898_A/T	chr6LG2	68,269,898	2.07E-09	0.157	0.1
	Zhongwan 6	PsZW6_chr6_85085481_A/T	chr6	85,085,481	6.80E-09	0.147	0.1

Table 2 Summary of the broad sense, genomic and missing heritabilities (H^2), prediction abilities from the whole-genome regression model, and proportion of variance explained (PVE) by the most significantly associated marker from the genome wide association model (GWAS) for plant height, shoot and root dry weight (SDW and RDW), plant emergence and root rot index (RRI) under naturally infested (NS), sterilized soil conditions (S), or the ratio between NS/S conditions. These results were obtained using the reference genome of cv. 'Caméor' and 'Zhongwan 6'. The mean and standard deviation (SD) of prediction abilities were calculated from Pearson's correlation coefficients between observed and predicted values of the validation subset (30%) in a cross-validation process repeated 50 times.

Trait	Broad sense heritab
Plant height $_{NS}$	0.96
Plant height $_{S}$	0.98
SDW_{NS}	0.92
SDW_{S}	0.92
$SDW_{NS/S}$	0.51
RRI_{NS}	0.43
Plant emergence $_{NS}$	0.89
RDW / SDW_{NS}	0.48

These values were originally reported by Wille et al. (2020) and are included here for comparison.

not-yet-known not-yet-known

not-yet-known

unknown

Supplementary material

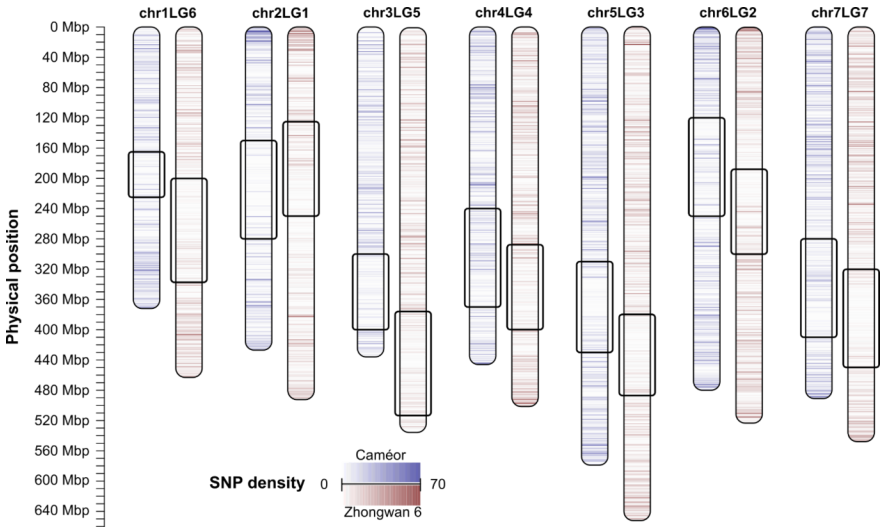

Supplementary Figure 1 Heatmap for the density of single nucleotide polymorphisms (SNPs) along the seven chromosomes of the reference genomes of Pisum sativum L. cv. 'Caméor' (blue) and 'Zhongwan' 6 (red), identified by genotyping-by-sequencing. Each color band represents a region of 1 Mbp and its color intensity represents the SNP density. The inner black rectangles on each chromosome represent the boundaries of the centromeric regions as defined by Kreplak et al. (2019) and Yang et al. (2022).

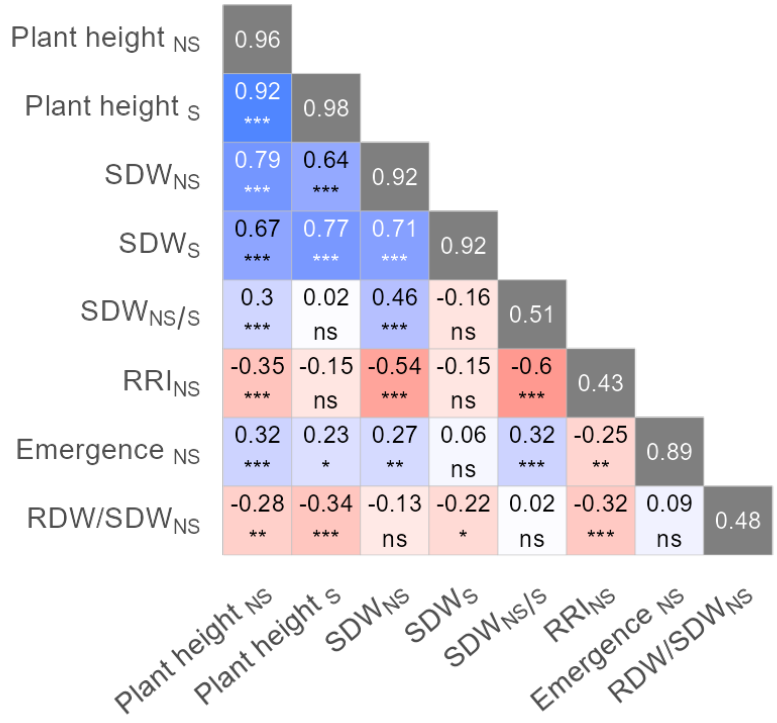

Supplementary Figure 2 Phenotypic correlations between adjusted means of the traits plant height, shoot and root dry weight (SDW and RDW), plant emergence and root rot index (RRI) under naturally infested (NS), sterilized soil conditions (S), the ratio between NS/S conditions, and the ratio between root and shoot dry weight (RDW/SDW) under NS conditions. The broad sense heritabilities are indicated within the main diagonal with gray background for each trait. Significance of correlations indicated as ***: $p < .0001$; **:$p < .001$; *: $p < .01$; ns: not significant.

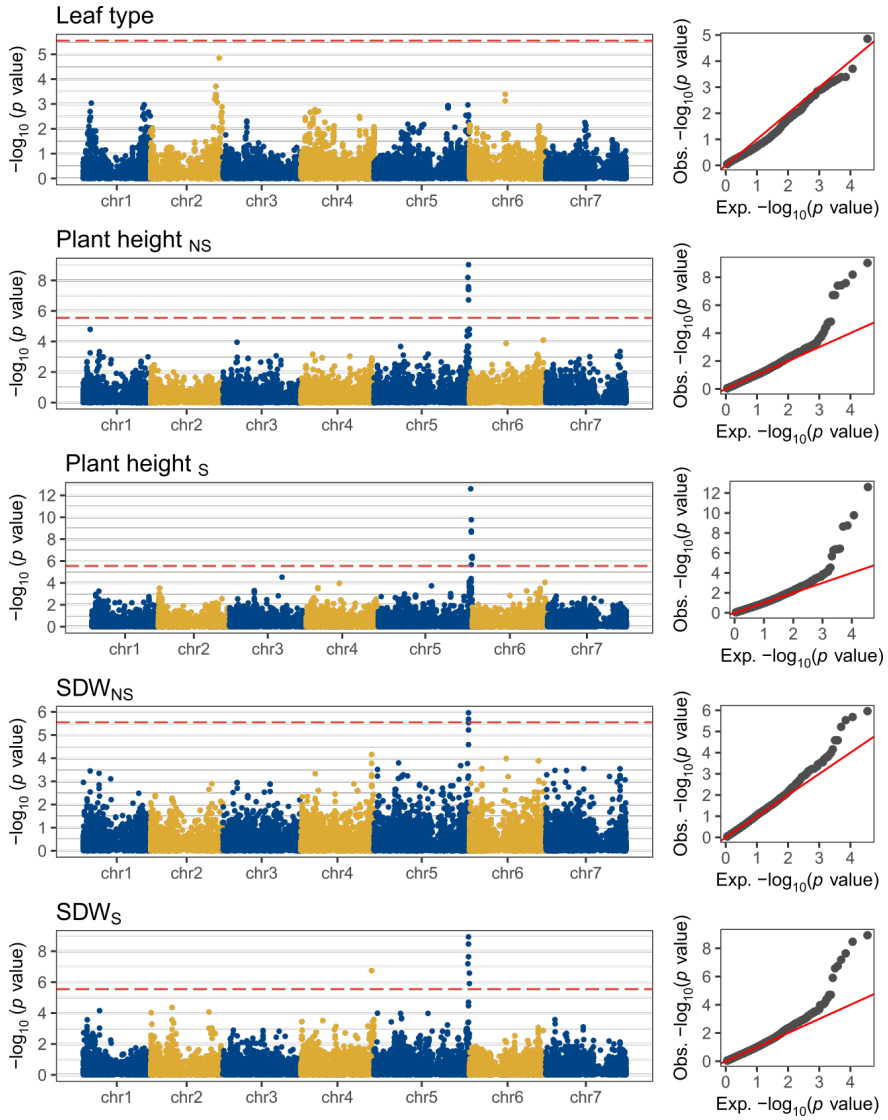

Supplementary Figure 3 Results of the genome-wide association studies for the traits leaf type, plant height and shoot dry weight (SDW) under naturally infested (NS) or sterilized soil conditions (S). The horizontal, red-dashed line represents the Bonferroni-corrected threshold, which was calculated with a genome-wide type I error rate $\alpha = 0.05$ ($p < 2.028 \times 10^{-6}$). The results are presented as individual Manhattan plots showing the significance of the sequence variants (SNP) and their physical location on each of the seven chromosomes of the reference genome of the cv. 'Zhongwan 6'. The corresponding quantile-quantile-plots to the right compare the deviation between the observed and the expected significance of the SNP from a theoretical X^2 distribution.

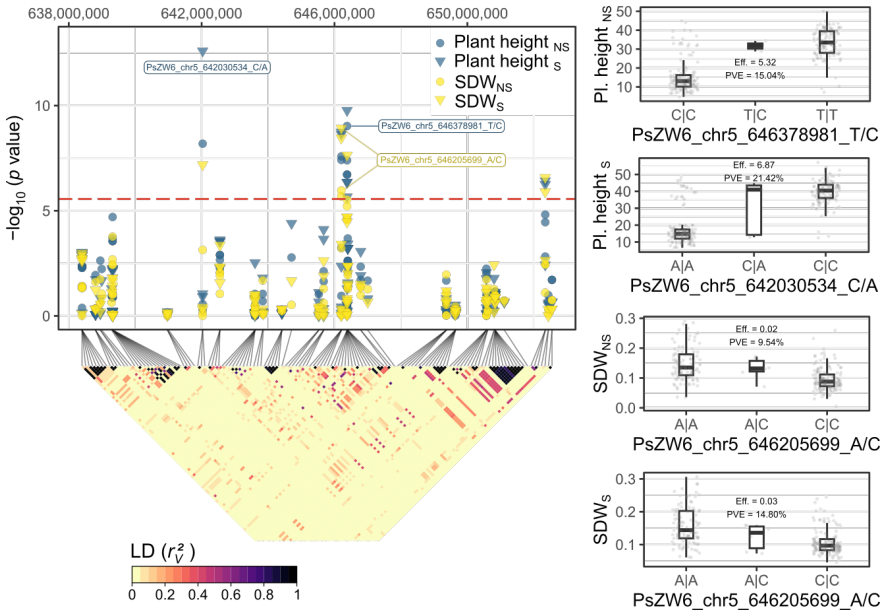

Supplementary Figure 4 Genetic dissection of the region of association on chromosome chr5LG3 for the traits plant height and shoot dry weight (SDW) under naturally infested (NS) and sterilized (S) soil conditions. The scatterplot shows combined results of individual genome wide association studies (GWAS). Each point shows the significance of sequence variants (SNP) and their physical location on chr5LG3 of the genome of cv. 'Zhongwan 6'. The horizontal, red-dashed line represents the Bonferroni-corrected threshold, which was calculated with a genome-wide type I error rate $\alpha = 0.05$ ($p < 2.028 \times 10^{-6}$). The tagged points indicate the most significant SNPs for each trait. The colored square matrix below represents the pairwise linkage disequilibrium (LD) measurements (r^2) between each pair of SNPs in the region of association. The boxplots show the distribution of phenotypic values between the genotypes of the most significant SNPs on chr5LG3. Each plot includes the marker effect (Eff.) and the proportion of variance (PVE) derived from the GWAS model.

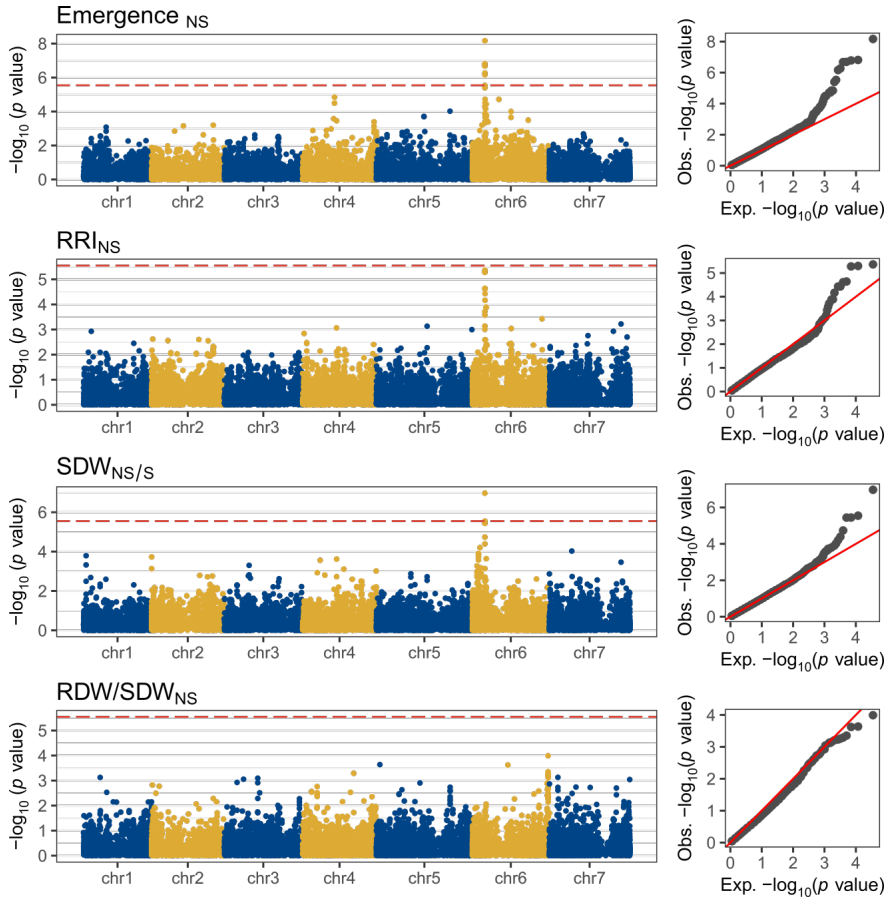

Supplementary Figure 5 Results of the genome-wide association studies for the root rot-related traits plant emergence and root rot index (RRI) under naturally infested soil conditions (NS), shoot dry weight (SDW) ratio between naturally infested and sterilized soil conditions (NS/S), and the ratio between root and shoot dry weight (RDW/SDW) under NS conditions. The horizontal, red-dashed line represents the Bonferroni-corrected threshold, which was calculated with a genome-wide type I error rate $\alpha = 0.05$ ($p < 2.028 \times 10^{-6}$). The results are presented as individual Manhattan plots showing the significance of the sequence variants (SNP) and their physical location on each of the seven chromosomes of the reference genome of the accession 'Zhongwan 6'. The corresponding quantile-quantile-plots to the right compare the deviation between the observed and the expected significance of the SNP from a theoretical X^2 distribution.

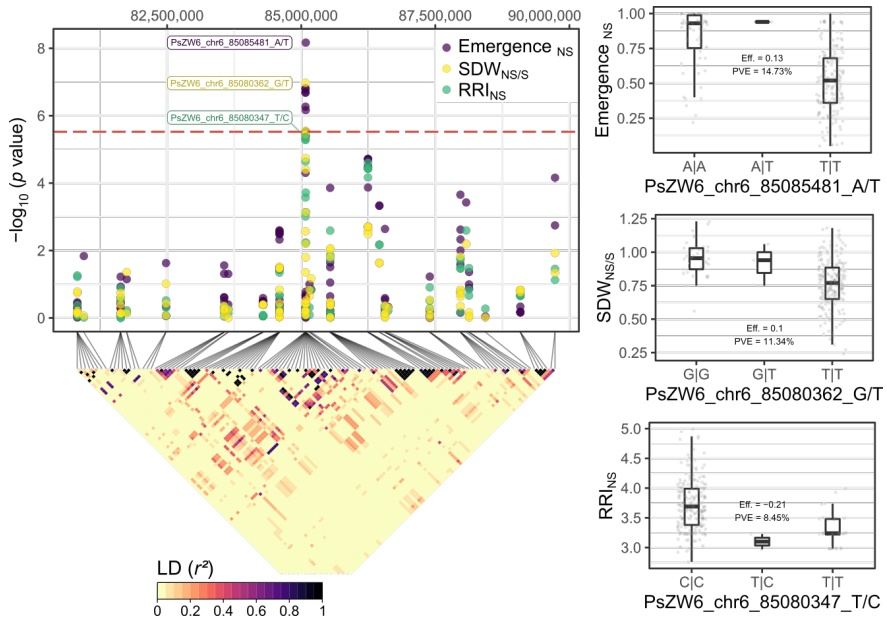

Supplementary Figure 6 Genetic dissection of the region of association on chromosome chr6LG2 for the root rot-related traits plant emergence, root rot index and shoot dry weight (SDW) under naturally infested (NS) and sterilized (S) soil conditions. The scatterplot shows combined results of individual genome wide association studies (GWAS). Each point shows the significance of sequence variants (SNP) and their physical location on chr6LG2 in the genome of cv. 'Zhongwan 6'. The horizontal, red-dashed line represents the Bonferroni-corrected threshold, which was calculated with a genome-wide type I error rate $\alpha = 0.05$ ($p < 2.028 \times 10^{-6}$). The tagged points indicate the most significant SNPs for each trait. The colored square matrix below represents the pairwise linkage disequilibrium (LD) measurements (r^2) between each pair of SNPs in the region of association. The boxplots show the distribution of phenotypic values between the genotypes of the most significant SNPs on chr5LG3. Each plot includes the marker effect (Eff.) and the proportion of variance (PVE) derived from the GWAS model.

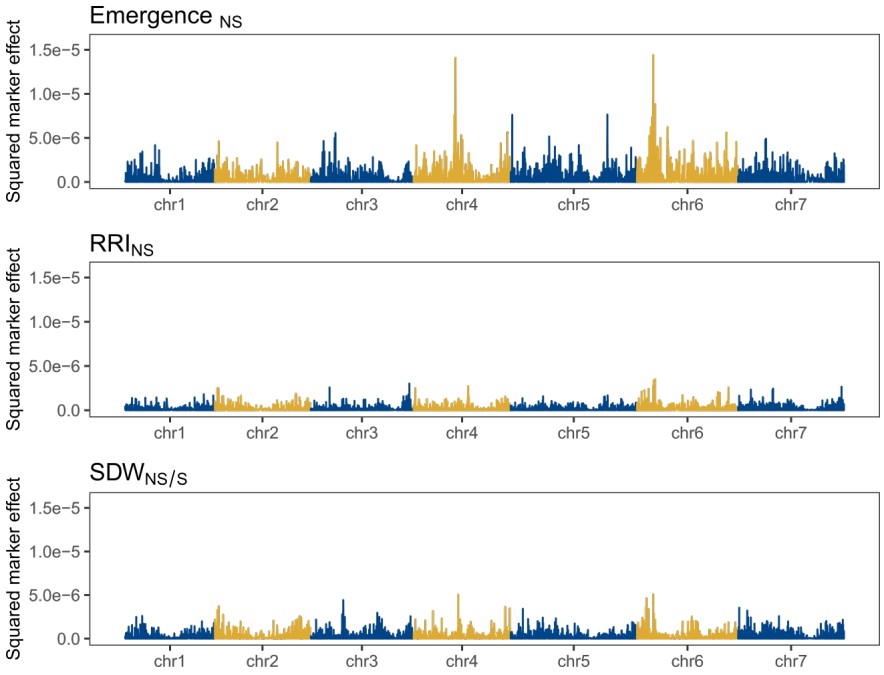

Supplementary Figure 7 Single nucleotide polymorphism (SNP) effects derived from a Bayes ridge regression model that used all SNP markers as predictors of root rot-related traits plant emergence and root rot index (RRI) under naturally infested soil conditions (NS), shoot dry weight (SDW) ratio between naturally infested and sterilized soil conditions (NS/S). The squared marker effects are plotted along their physical position on each one of the seven chromosomes of the reference genome 'Zhongwan 6'.

Supplementary Table 1 List of plant material and phenotypic data used in this study, originally reported by Wille et al. (2020). Raw genotypic data for each genotype were deposited in the NCBI Sequence Read Archive (SRA) under the corresponding BioSample and SRA run identifiers. The traits plant height, shoot and root dry weight (SDW and RDW), plant emergence and root rot index (RRI) were evaluated under naturally infested (NS) or sterilized (S) soil conditions, where NS/S indicates the ratio between them.

Supplementary Table 2 Results of the genome-wide association studies for leaf type, plant height, shoot and root dry weight (SDW and RDW, respectively), plant emergence and root rot index (RRI) evaluated under naturally infested or sterilized soil conditions (NS and S, respectively). PVE indicates the proportion of explained variance from each marker, while Est. Effect indicates the estimated effect of the sequence variant. The annotation was obtained with the software snpEff, using the coding regions annotated in the reference genome of the cv. 'Caméor' and 'Zhongwan 6'.

References

Bai, B., Liu, W., Qiu, X., Zhang, J., Zhang, J., & Bai, Y. (2022). The root microbiome: Community assembly and its contributions to plant fitness. *Journal of Integrative Plant Biology* , jipb.13226. https://doi.org/10.1111/jipb.13226

Bari, Md. A. A., Zheng, P., Viera, I., Worral, H., Szwiec, S., Ma, Y., Main, D., Coyne, C. J., McGee, R. J., & Bandillo, N. (2021). Harnessing Genetic Diversity in the USDA Pea Germplasm Collection Through Genomic Prediction. *Frontiers in Genetics* , *12* , 707754. https://doi.org/10.3389/fgene.2021.707754

Bodah, E. T., Porter, L. D., Chaves, B., & Dhingra, A. (2016). Evaluation of pea accessions and commercial

cultivars for fusarium root rot resistance. *Euphytica* , *208* (1), 63–72. https://doi.org/10.1007/s10681-015-1545-6

Bonhomme, M., André, O., Badis, Y., Ronfort, J., Burgarella, C., Chantret, N., Prosperi, J., Briskine, R., Mudge, J., Debéllé, F., Navier, H., Miteul, H., Hajri, A., Baranger, A., Tiffin, P., Dumas, B., Pilet-Nayel, M., Young, N. D., & Jacquet, C. (2014). High-density genome-wide association mapping implicates an F -box encoding gene in *M edicago truncatula* resistance to*A phanomyces euteiches* . *New Phytologist* ,*201* (4), 1328–1342. https://doi.org/10.1111/nph.12611

Browning, B. L., Zhou, Y., & Browning, S. R. (2018). A One-Penny Imputed Genome from Next-Generation Reference Panels. *The American Journal of Human Genetics* , *103* (3), 338–348. https://doi.org/10.1016/j.ajhg.2018.07.015

Burstin, J., Marget, P., Huart, M., Moessner, A., Mangin, B., Duchene, C., Desprez, B., Munier-Jolain, N., & Duc, G. (2007). Developmental Genes Have Pleiotropic Effects on Plant Morphology and Source Capacity, Eventually Impacting on Seed Protein Content and Productivity in Pea.*Plant Physiology* , *144* (2), 768–781. https://doi.org/10.1104/pp.107.096966

Catchen, J., Hohenlohe, P. A., Bassham, S., Amores, A., & Cresko, W. A. (2013). Stacks: An analysis tool set for population genomics.*Molecular Ecology* , *22* (11), 3124–3140. https://doi.org/10.1111/mec.12354

Chen, H., Wang, C., Conomos, M. P., Stilp, A. M., Li, Z., Sofer, T., Szpiro, A. A., Chen, W., Brehm, J. M., Celedon, J. C., Redline, S., Papanicolaou, G. J., Thornton, T. A., Laurie, C. C., Rice, K., & Lin, X. (2016). Control for Population Structure and Relatedness for Binary Traits in Genetic Association Studies via Logistic Mixed Models.*American Journal of Human Genetics* , *98* (4), 653–666. https://doi.org/10.1016/j.ajhg.2016.02.012

Chiang, C. C., & Hadwiger, L. A. (1991). The *Fusarium solani* -Induced Expression of a Pea Gene Family Encoding High Cysteine Content Proteins. *Molecular Plant-Microbe Interactions* , *4* (4), 324–331. https://doi.org/10.1094/MPMI-4-324

Cingolani, P., Platts, A., Wang, L. L., Coon, M., Nguyen, T., Wang, L., Land, S. J., Lu, X., & Ruden, D. M. (2012). A program for annotating and predicting the effects of single nucleotide polymorphisms, SnpEff: SNPs in the genome of Drosophila melanogaster strain w1118; iso-2; iso-3. *Fly* , *6* (2), 80–92. https://doi.org/10.4161/fly.19695

Colston-Nepali, L., Tigano, A., Boyle, B., & Friesen, V. (2019). Hybridization does not currently pose conservation concerns to murres in the Atlantic. *Conservation Genetics* , *20* (6), 1465–1470. https://doi.org/10.1007/s10592-019-01223-y

Conner, R. L., Chang, K. F., Hwang, S. F., Warkentin, T. D., & McRae, K. B. (2013). Assessment of tolerance for reducing yield losses in field pea caused by Aphanomyces root rot. *Canadian Journal of Plant Science* , *93* (3), 473–482. https://doi.org/10.4141/cjps2012-183

Cowger, C., & Brown, J. K. M. (2019). Durability of Quantitative Resistance in Crops: Greater Than We Know? *Annual Review of Phytopathology* , *57* (1), 253–277. https://doi.org/10.1146/annurev-phyto-082718-100016

Coyne, C. J., Pilet-Nayel, M.-L., McGee, R. J., Porter, L. D., Smykal, P., & Grunwald, N. J. (2015). Identification of QTL controlling high levels of partial resistance to *Fusarium solani* f. Sp.*Pisi* in pea. *Plant Breeding* , *134* (4), 446–453. https://doi.org/10.1111/pbr.12287

Coyne, C. J., Porter, L. D., Boutet, G., Ma, Y., McGee, R. J., Lesne, A., Baranger, A., & Pilet-Nayel, M.-L. (2019). Confirmation of Fusarium root rot resistance QTL Fsp-Ps 2.1 of pea under controlled conditions.*BMC Plant Biology* , *19* (1), 98. https://doi.org/10.1186/s12870-019-1699-9

Cusworth, G., Garnett, T., & Lorimer, J. (2021). Legume dreams: The contested futures of sustainable plant-based food systems in Europe.*Global Environmental Change* , *69* , 102321. https://doi.org/10.

1016/j.gloenvcha.2021.102321

de los Campos, G., Sorensen, D., & Gianola, D. (2015). Genomic Heritability: What Is It? *PLOS Genetics* , *11* (5), e1005048. https://doi.org/10.1371/journal.pgen.1005048

Desgroux, A., Baudais, V. N., Aubert, V., Le Roy, G., de Larambergue, H., Miteul, H., Aubert, G., Boutet, G., Duc, G., Baranger, A., Burstin, J., Manzanares-Dauleux, M., Pilet-Nayel, M.-L., & Bourion, V. (2018). Comparative Genome-Wide-Association Mapping Identifies Common Loci Controlling Root System Architecture and Resistance to Aphanomyces euteiches in Pea. *Frontiers in Plant Science* , *8* , 2195. https://doi.org/10.3389/fpls.2017.02195

Diaz, L. M., Arredondo, V., Ariza-Suarez, D., Aparicio, J., Buendia, H. F., Cajiao, C., Mosquera, G., Beebe, S. E., Mukankusi, C. M., Raatz, B., & Diaz, L. M. (2021). Genetic Analyses and Genomic Predictions of Root Rot Resistance in Common Bean Across Trials and Populations.*Frontiers in Plant Science* , *12* (March), 1–15. https://doi.org/10.3389/fpls.2021.629221

Ellis, T. H., Turner, L., Hellens, R. P., Lee, D., Harker, C. L., Enard, C., Domoney, C., & Davies, D. R. (1992). Linkage maps in pea.*Genetics* , *130* (3), 649–663. https://doi.org/10.1093/genetics/130.3.649

Engelhardt, S., Trutzenberg, A., & Huckelhoven, R. (2020). Regulation and Functions of ROP GTPases in Plant–Microbe Interactions.*Cells* , *9* (9), 2016. https://doi.org/10.3390/cells9092016

FAO. (2024). *Food and Agriculture Organization* . FAOSTAT Statistical Database. https://www.fao.org/faostat

Gali, K. K., Sackville, A., Tafesse, E. G., Lachagari, V. B. R., McPhee, K., Hybl, M., Mikić, A., Smýkal, P., McGee, R., Burstin, J., Domoney, C., Ellis, T. H. N., Tar'an, B., & Warkentin, T. D. (2019). Genome-Wide Association Mapping for Agronomic and Seed Quality Traits of Field Pea (Pisum sativum L.). *Frontiers in Plant Science* , *10* , 1538. https://doi.org/10.3389/fpls.2019.01538

Gogarten, S. M., Sofer, T., Chen, H., Yu, C., Brody, J. A., Thornton, T. A., Rice, K. M., & Conomos, M. P. (2019). Genetic association testing using the GENESIS R/Bioconductor package. *Bioinformatics* ,*35* (24), 5346–5348. https://doi.org/10.1093/bioinformatics/btz567

Gossen, B. D., Conner, R. L., Chang, K.-F., Pasche, J. S., McLaren, D. L., Henriquez, M. A., Chatterton, S., & Hwang, S.-F. (2016). Identifying and Managing Root Rot of Pulses on the Northern Great Plains. *Plant Disease* , *100* (10), 1965–1978. https://doi.org/10.1094/PDIS-02-16-0184-FE

Hamon, C., Baranger, A., Coyne, C. J., McGee, R. J., Le Goff, I., L'Anthoëne, V., Esnault, R., Rivière, J.-P., Klein, A., Mangin, P., McPhee, K. E., Roux-Duparque, M., Porter, L., Miteul, H., Lesné, A., Morin, G., Onfroy, C., Moussart, A., Tivoli, B., ... Pilet-Nayel, M.-L. (2011). New consistent QTL in pea associated with partial resistance to Aphanomyces euteiches in multiple French and American environments. *Theoretical and Applied Genetics* , *123* (2), 261–281. https://doi.org/10.1007/s00122-011-1582-z

Hamon, C., Coyne, C. J., McGee, R. J., Lesné, A., Esnault, R., Mangin, P., Hervé, M., Le Goff, I., Deniot, G., Roux-Duparque, M., Morin, G., McPhee, K. E., Delourme, R., Baranger, A., & Pilet-Nayel, M.-L. (2013). QTL meta-analysis provides a comprehensive view of loci controlling partial resistance to Aphanomyces euteichesin four sources of resistance in pea. *BMC Plant Biology* , *13* (1), 45. https://doi.org/10.1186/1471-2229-13-45

Jayasekaran, K., Kim, K.-N., Vivekanandan, M., Shin, J. S., & Ok, S. H. (2006). Novel calcium-binding GTPase (AtCBG) involved in ABA-mediated salt stress signaling in Arabidopsis. *Plant Cell Reports* ,*25* (11), 1255–1262. https://doi.org/10.1007/s00299-006-0195-5

Jha, A. B., Gali, K. K., Alam, Z., Lachagari, V. B. R., & Warkentin, T. D. (2021). Potential Application of Genomic Technologies in Breeding for Fungal and Oomycete Disease Resistance in Pea. *Agronomy* ,*11* (6), Article 6. https://doi.org/10.3390/agronomy11061260

Kälin, C., Piombo, E., Bourras, S., Brantestam, A. K., Dubey, M., Elfstrand, M., & Karlsson, M. (2024). Transcriptomic analysis identifies candidate genes for Aphanomyces root rot disease resistance in pea. *BMC Plant Biology* , *24* (1), 144. https://doi.org/10.1186/s12870-024-04817-y

Kawano, Y., Kaneko-Kawano, T., & Shimamoto, K. (2014). Rho family GTPase-dependent immunity in plants and animals. *Frontiers in Plant Science* , *5* . https://doi.org/10.3389/fpls.2014.00522

Kiirika, L. M., Bergmann, H. F., Schikowsky, C., Wimmer, D., Korte, J., Schmitz, U., Niehaus, K., & Colditz, F. (2012). Silencing of the Rac1 GTPase *MtROP9* in *Medicago truncatula* Stimulates Early Mycorrhizal and Oomycete Root Colonizations But Negatively Affects Rhizobial Infection. *Plant Physiology* , *159* (1), 501–516. https://doi.org/10.1104/pp.112.193706

Klein, A., Houtin, H., Rond, C., Marget, P., Jacquin, F., Boucherot, K., Huart, M., Rivière, N., Boutet, G., Lejeune-Hénaut, I., & Burstin, J. (2014). QTL analysis of frost damage in pea suggests different mechanisms involved in frost tolerance. *Theoretical and Applied Genetics* , *127* (6), 1319–1330. https://doi.org/10.1007/s00122-014-2299-6

Kreplak, J., Madoui, M.-A., Cápal, P., Novák, P., Labadie, K., Aubert, G., Bayer, P. E., Gali, K. K., Syme, R. A., Main, D., Klein, A., Bérard, A., Vrbová, I., Fournier, C., d'Agata, L., Belser, C., Berrabah, W., Toegelová, H., Milec, Z., ... Burstin, J. (2019). A reference genome for pea provides insight into legume genome evolution.*Nature Genetics* , *51* (9), 1411–1422. https://doi.org/10.1038/s41588-019-0480-1

Lamesch, P., Berardini, T. Z., Li, D., Swarbreck, D., Wilks, C., Sasidharan, R., Muller, R., Dreher, K., Alexander, D. L., Garcia-Hernandez, M., Karthikeyan, A. S., Lee, C. H., Nelson, W. D., Ploetz, L., Singh, S., Wensel, A., & Huala, E. (2012). The Arabidopsis Information Resource (TAIR): Improved gene annotation and new tools.*Nucleic Acids Research* , *40* (D1), D1202–D1210. https://doi.org/10.1093/nar/gkr1090

Lamichhane, J. R., Dürr, C., Schwanck, A. A., Robin, M.-H., Sarthou, J.-P., Cellier, V., Messéan, A., & Aubertot, J.-N. (2017). Integrated management of damping-off diseases. A review. *Agronomy for Sustainable Development* , *37* (2), 10. https://doi.org/10.1007/s13593-017-0417-y

Langmead, B., & Salzberg, S. L. (2012). Fast gapped-read alignment with Bowtie 2. *Nature Methods* , *9* (4), 357–359. https://doi.org/10.1038/nmeth.1923

Lavaud, C., Lesné, A., Leprévost, T., & Pilet-Nayel, M.-L. (2024). Fine mapping of Ae-Ps4.5, a major locus for resistance to pathotype III of Aphanomyces euteiches in pea. *Theoretical and Applied Genetics* ,*137* (2), 47. https://doi.org/10.1007/s00122-024-04548-6

Lavaud, C., Lesné, A., Piriou, C., Le Roy, G., Boutet, G., Moussart, A., Poncet, C., Delourme, R., Baranger, A., & Pilet-Nayel, M.-L. (2015). Validation of QTL for resistance to Aphanomyces euteiches in different pea genetic backgrounds using near-isogenic lines. *Theoretical and Applied Genetics* , *128* (11), 2273–2288. https://doi.org/10.1007/s00122-015-2583-0

Legarra, A., Ricard, A., & Varona, L. (2018). GWAS by GBLUP: Single and Multimarker EMMAX and Bayes Factors, with an Example in Detection of a Major Gene for Horse Gait. *G3 Genes|Genomes|Genetics* , *8* (7), 2301–2308. https://doi.org/10.1534/g3.118.200336

Leprévost, T., Boutet, G., Lesné, A., Rivière, J.-P., Vetel, P., Glory, I., Miteul, H., Le Rat, A., Dufour, P., Regnault-Kraut, C., Sugio, A., Lavaud, C., & Pilet-Nayel, M.-L. (2023). Advanced backcross QTL analysis and comparative mapping with RIL QTL studies and GWAS provide an overview of QTL and marker haplotype diversity for resistance to Aphanomyces root rot in pea (Pisum sativum). *Frontiers in Plant Science* , *14* , 1189289. https://doi.org/10.3389/fpls.2023.1189289

Mangin, B., Siberchicot, A., Nicolas, S., Doligez, A., This, P., & Cierco-Ayrolles, C. (2012). Novel measures of linkage disequilibrium that correct the bias due to population structure and relatedness.*Heredity* , *108* (3), 285–291. https://doi.org/10.1038/hdy.2011.73

Martin, D. N., Proebsting, W. M., & Hedden, P. (1997). Mendel's dwarfing gene: cDNAs from the *Le* alleles and function of the expressed proteins. *Proceedings of the National Academy of Sciences* , *94* (16), 8907–8911. https://doi.org/10.1073/pnas.94.16.8907

Mendel, G. (1866). *Versuche über Pflanzenhybriden* . Vieweg+Teubner Verlag. https://doi.org/10.1007/978-3-663-19714-0

Mikić, A., Mihailović, V., Ćupina, B., Kosev, V., Warkentin, T., Mcphee, K., Ambrose, M., Hofer, J., & Ellis, N. (2011). Genetic background and agronomic value of leaf types in pea (Pisum sativum). *Ratarstvo i Povrtarstvo* , *48* (2), 275–284. https://doi.org/10.5937/ratpov1102275M

Nelson, R., Wiesner-Hanks, T., Wisser, R., & Balint-Kurti, P. (2018). Navigating complexity to breed disease-resistant crops. *Nature Reviews. Genetics* , *19* (1), 21–33. https://doi.org/10.1038/nrg.2017.82

Oldach, K. H., Peck, D. M., Nair, R. M., Sokolova, M., Harris, J., Bogacki, P., & Ballard, R. (2014). Genetic analysis of tolerance to the root lesion nematode Pratylenchus neglectus in the legume Medicago littoralis. *BMC Plant Biology* , *14* (1), 100. https://doi.org/10.1186/1471-2229-14-100

Pandey, A. K., Rubiales, D., Wang, Y., Fang, P., Sun, T., Liu, N., & Xu, P. (2021). Omics resources and omics-enabled approaches for achieving high productivity and improved quality in pea (Pisum sativum L.). *Theoretical and Applied Genetics* , *134* (3), 755–776. https://doi.org/10.1007/s00122-020-03751-5

Pérez, P., & De Los Campos, G. (2014). Genome-wide regression and prediction with the BGLR statistical package. *Genetics* ,*198* (2), 483–495. https://doi.org/10.1534/genetics.114.164442

Pilet-Nayel, M.-L., Moury, B., Caffier, V., Montarry, J., Kerlan, M.-C., Fournet, S., Durel, C.-E., & Delourme, R. (2017). Quantitative Resistance to Plant Pathogens in Pyramiding Strategies for Durable Crop Protection. *Frontiers in Plant Science* , *8* , 1838. https://doi.org/10.3389/fpls.2017.01838

Poland, J. A., Brown, P. J., Sorrells, M. E., & Jannink, J.-L. (2012). Development of High-Density Genetic Maps for Barley and Wheat Using a Novel Two-Enzyme Genotyping-by-Sequencing Approach. *PLoS ONE* ,*7* (2), e32253. https://doi.org/10.1371/journal.pone.0032253

Ramsay, L., Koh, C. S., Kagale, S., Gao, D., Kaur, S., Haile, T., Gela, T. S., Chen, L.-A., Cao, Z., Konkin, D. J., Toegelová, H., Doležel, J., Rosen, B. D., Stonehouse, R., Humann, J. L., Main, D., Coyne, C. J., McGee, R. J., Cook, D. R., … Bett, K. E. (2021). *Genomic rearrangements have consequences for introgression breeding as revealed by genome assemblies of wild and cultivated lentil species* . https://doi.org/10.1101/2021.07.23.453237

Rivero, C., Traubenik, S., Zanetti, M. E., & Blanco, F. A. (2019). Small GTPases in plant biotic interactions. *Small GTPases* ,*10* (5), 350–360. https://doi.org/10.1080/21541248.2017.1333557

Rubiales, D., Barilli, E., & Rispail, N. (2023). Breeding for Biotic Stress Resistance in Pea. *Agriculture* , *13* (9), 1825. https://doi.org/10.3390/agriculture13091825

Rubiales, D., González-Bernal, M. J., Warkentin, T., Bueckert, R., Vaz Patto, M. C., McPhee, K., McGee, R., & Smýkal, P. (2019). Advances in pea breeding. In G. Hochmuth (Ed.), *Achieving sustainable cultivation of vegetables* (1st ed., pp. 575–606). Burleigh Dodds Science Publishing. https://doi.org/10.1201/9780429275456

Shehata, M. A., Davis, D. W., & Pfleger, F. L. (1983). Breeding for Resistance to Aphanomyces euteiches Root Rot and Rhizoctonia solani Stem Rot in Peas. *Journal of the American Society for Horticultural Science* , *108* (6), 1080–1085. https://doi.org/10.21273/JASHS.108.6.1080

Sinjushin, A., Semenova, E., & Vishnyakova, M. (2022). Usage of Morphological Mutations for Improvement of a Garden Pea (Pisum sativum): The Experience of Breeding in Russia. *Agronomy* , *12* (3), Article 3. https://doi.org/10.3390/agronomy12030544

Tang, H., Krishnakumar, V., Bidwell, S., Rosen, B., Chan, A., Zhou, S., Gentzbittel, L., Childs, K. L., Yandell, M., Gundlach, H., Mayer, K. F., Schwartz, D. C., & Town, C. D. (2014). An improved genome release (version Mt4.0) for the model legume Medicago truncatula. *BMC Genomics* , *15* (1), 312. https://doi.org/10.1186/1471-2164-15-312

Tayeh, N., Aubert, G., Pilet-Nayel, M.-L., Lejeune-Hénaut, I., Warkentin, T. D., & Burstin, J. (2015). Genomic Tools in Pea Breeding Programs: Status and Perspectives. *Frontiers in Plant Science* ,*6* . https://doi.org/10.3389/fpls.2015.01037

Tayeh, N., Hofer, J. M. I., Aubert, G., Jacquin, F., Turner, L., Kreplak, J., Paajanen, P., Le Signor, C., Dalmais, M., Pflieger, S., Geffroy, V., Ellis, N., & Burstin, J. (2024). *Afila* , the origin and nature of a major innovation in the history of pea breeding.*New Phytologist* , nph.19800. https://doi.org/10.1111/nph.19800

Tello, D., Gonzalez-Garcia, L. N., Gomez, J., Zuluaga-Monares, J. C., Garcia, R., Angel, R., Mahecha, D., Duarte, E., Leon, M. D. R., Reyes, F., Escobar-Velasquez, C., Linares-Vasquez, M., Cardozo, N., & Duitama, J. (2023). NGSEP4: Efficient and accurate identification of orthogroups and whole-genome alignment. *Molecular Ecology Resources* ,*23* (3), 712–724. https://doi.org/10.1111/1755-0998.13737

Wang, Y., Zhang, W.-Z., Song, L.-F., Zou, J.-J., Su, Z., & Wu, W.-H. (2008). Transcriptome Analyses Show Changes in Gene Expression to Accompany Pollen Germination and Tube Growth in Arabidopsis. *Plant Physiology* , *148* (3), 1201–1211. https://doi.org/10.1104/pp.108.126375

White, R. R., Lin, C., Leaves, I., Castro, I. G., Metz, J., Bateman, B. C., Botchway, S. W., Ward, A. D., Ashwin, P., & Sparkes, I. (2020). Miro2 tethers the ER to mitochondria to promote mitochondrial fusion in tobacco leaf epidermal cells. *Communications Biology* ,*3* (1), 161. https://doi.org/10.1038/s42003-020-0872-x

Wille, L., Messmer, M. M., Bodenhausen, N., Studer, B., & Hohmann, P. (2020). Heritable Variation in Pea for Resistance Against a Root Rot Complex and Its Characterization by Amplicon Sequencing. *Frontiers in Plant Science* , *11* , 542153. https://doi.org/10.3389/fpls.2020.542153

Wille, L., Messmer, M. M., Studer, B., & Hohmann, P. (2019). Insights to plant-microbe interactions provide opportunities to improve resistance breeding against root diseases in grain legumes. *Plant, Cell & Environment* , *42* (1), 20–40. https://doi.org/10.1111/pce.13214

Williamson-Benavides, B. A., Sharpe, R. M., Nelson, G., Bodah, E. T., Porter, L. D., & Dhingra, A. (2021). Identification of Root Rot Resistance QTLs in Pea Using Fusarium solani f. Sp. Pisi-Responsive Differentially Expressed Genes. *Frontiers in Genetics* , *12* , 629267. https://doi.org/10.3389/fgene.2021.629267

Wohor, O. Z., Rispail, N., Ojiewo, C. O., & Rubiales, D. (2022). Pea Breeding for Resistance to Rhizospheric Pathogens. *Plants* ,*11* (19), 2664. https://doi.org/10.3390/plants11192664

Wu, L., Fredua-Agyeman, R., Hwang, S.-F., Chang, K.-F., Conner, R. L., McLaren, D. L., & Strelkov, S. E. (2021). Mapping QTL associated with partial resistance to Aphanomyces root rot in pea (Pisum sativum L.) using a 13.2 K SNP array and SSR markers. *Theoretical and Applied Genetics* , *134* (9), Article 9. https://doi.org/10.1007/s00122-021-03871-6

Wu, L., Fredua-Agyeman, R., Strelkov, S. E., Chang, K.-F., & Hwang, S.-F. (2022). Identification of Quantitative Trait Loci Associated With Partial Resistance to Fusarium Root Rot and Wilt Caused by Fusarium graminearum in Field Pea. *Frontiers in Plant Science* , *12* , 784593. https://doi.org/10.3389/fpls.2021.784593

Yamaoka, S., & Leaver, C. J. (2008). EMB2473/MIRO1, an*Arabidopsis* Miro GTPase, Is Required for Embryogenesis and Influences Mitochondrial Morphology in Pollen. *The Plant Cell* ,*20* (3), 589–601. https://doi.org/10.1105/tpc.107.055756

Yang, T., Liu, R., Luo, Y., Hu, S., Wang, D., Wang, C., Pandey, M. K., Ge, S., Xu, Q., Li, N., Li, G., Huang, Y., Saxena, R. K., Ji, Y., Li, M., Yan, X., He, Y., Liu, Y., Wang, X., ... Zong, X. (2022). Improved pea reference genome and pan-genome highlight genomic features and evolutionary characteristics. *Nature Genetics* . https://doi.org/10.1038/s41588-022-01172-2

Yuan, Z., Xie, X., Liu, M., He, Y., & He, L. (2024). Mutations of*PsPALM1a* and *PsPALM1b* associated with the *afila* phenotype in Pea. *Physiologia Plantarum* ,*176* (3), e14310. https://doi.org/10.1111/ppl.14310

Zander, P., Amjath-Babu, T. S., Preissel, S., Reckling, M., Bues, A., Schlafke, N., Kuhlman, T., Bachinger, J., Uthes, S., Stoddard, F., Murphy-Bokern, D., & Watson, C. (2016). Grain legume decline and potential recovery in European agriculture: A review. *Agronomy for Sustainable Development* , *36* (2), 26. https://doi.org/10.1007/s13593-016-0365-y

Zhang, J., Liu, F., Reif, J. C., & Jiang, Y. (2021). On the use of GBLUP and its extension for GWAS with additive and epistatic effects.*G3 Genes|Genomes|Genetics* , *11* (7), jkab122. https://doi.org/10.1093/g3journal/jkab122

Statements and Declarations

Funding

This study is part of the AGRIBIOME project funded by the Gebert Ruf Stiftung (project no. GRS-082/19), and the LIVESEED project: Improving the performance of organic agriculture by boosting organic seed and plant breeding efforts across Europe supported by the European Union's HORIZON 2020 Research and Innovation Program under the Grant Agreement No. 727230 , by the Swiss State Secretariat for Education, Research and Innovation (SERI) under contract number 17.0009, and by MICIU/AEI/10.13039/501100011033 and FSE+ under grant reference no RYC2022-037997-I. We would also like to thank the Mercator Research Program of the World Food System Center of ETH Zurich and the Swiss Federal Office for Agriculture (REF-1062- 22100) for supporting the previous project resPEAct, on which this study is based.

Competing interests

The authors declare that the research was conducted in the absence of any commercial or financial relationships that could be construed as a potential conflict of interest.

Author Contributions

Conception and design of the study: MM, PH, and BS. Funding acquisition: MM, PH, and BS. Material preparation, DNA extraction and sequencing: LW, PH, and MH. Data analysis: DAS. Writing – original draft preparation: DAS. Writing – review and editing: DAS, PH, VG, MS, MM and BS. All authors read and approved the final version of the manuscript.

Data availability

Raw sequencing data for the 254 pea genotypes are deposited in the NCBI Sequence Read Archive (SRA) under BioProject number PRJNA1127519. The genotypic matrices generated in this study using the Cam. and ZW6 reference genomes are deposited at the ETH Research Collection under doi.org/10.3929/ethz-b-000681298. These matrices are provided in compressed Variant Call Format (VCF) and Genomic Data Structure (GDS) formats. The phenotypic data used in this study were originally reported by Wille et al. (2020). These data are reproduced here in the Supplementary Table 1 and were also deposited in the same entry of the ETH Research Collection for reference.